An exact periodic-orbit formula for the energy levels of the three-pronged star graph

2009 J. Phys. A: Math. Theor. 42 135102

(http://iopscience.iop.org/1751-8121/42/13/135102)

IOP PUBLISHING JOURNAL OF PHYSICS A: MATHEMATICAL AND THEORETICAL

J. Phys. A: Math. Theor. **42** (2009) 135102 (18pp) doi:10.1088/1751-8113/42/13/135102

An exact periodic-orbit formula for the energy levels of the three-pronged star graph

Z S Pastore and R Blümel

Department of Physics, Wesleyan University, Middletown, CT 06459-0155, USA

Received 26 July 2008, in final form 13 January 2009
Published 9 March 2009
Online at stacks.iop.org/JPhysA/42/135102

Abstract
We derive an exact periodic-orbit expansion formula for the energy levels of the three-pronged star graph. In addition, we present a proof of the 'one-root-per-root-cell' property and derive exact periodic-orbit sum rules. A spin-off of our periodic-orbit formulae is novel arithmetic series for π^2.

PACS number: 03.65.Ge

1. Introduction

A graph is a network of edges and vertices, as shown in figure 1. A graph becomes a physical quantum graph [1–4] if we imagine a quantum particle roaming on the graph. The dynamics of the quantum particle is governed by the one-dimensional Schrödinger equation with the boundary conditions of flux conservation at internal vertices and Dirichlet, Neumann or mixed boundary conditions at the dead-end vertices of the graph.

At first glance, the graph in figure 1 looks like a stick molecule frequently used in chemistry as a model of large molecules. Accordingly, quantum graphs have been used in the past for computing various properties of molecules [5, 6]. Quantum graphs as a field of study took off about a decade ago when Kottos and Smilansky [1, 2] investigated them in the context of quantum chaos and complex systems. Quantum graphs, as models for complex quantum systems [7], are attractive from an analytical point of view since they allow many of their physical characteristics to be computed analytically and exactly. For instance, the level density of a quantum graph can be expressed exactly as a sum over the classical periodic orbits of the graph [1, 2].

About seven years ago it was discovered [8, 9] that for a class of quantum graphs, called 'regular', the energy levels themselves had exact periodic-orbit expansions. The very idea of periodic-orbit expansions of individual energy levels was new and opened a new direction in quantum graph research. Since then it was proved [10] that the direct expansion of energy levels into an exact periodic-orbit sum is possible for *all* quantum graphs, not just the 'regular' ones. However, the explicit construction of such expansions is difficult and to date has been accomplished only for some simple, linear (in the sense of non-branched) quantum graphs.

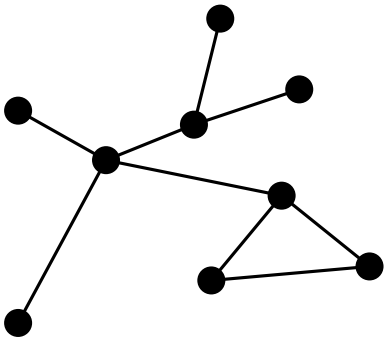

Figure 1. Example of a graph. Nine edges (lines) connect nine vertices (dots).

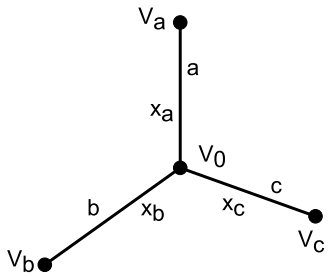

Figure 2. Three-pronged star graph with three edges of lengths a, b and c, three dead-end vertices V_a, V_b and V_c terminating the three edges a, b and c, respectively, and one central vertex V_0. The central vertex is the origin of three local coordinate systems with coordinates $0 \leqslant x_a \leqslant a$, $0 \leqslant x_b \leqslant b$, and $0 \leqslant x_c \leqslant c$.

Going beyond the case of 'regular' quantum graphs, the purpose of this paper is to provide exact periodic-orbit expansion formulae for the spectrum of the three-pronged star graph (see figure 2) for which the 'regularity condition' [8] is not satisfied. Therefore, the three-pronged star graph has not only a richer topology than the graphs studied before (it is branched), but also a more complex spectrum. Nevertheless, as we will show below, this quantum graph, too, can be solved explicitly.

Star graphs have been studied in the literature before [11–13]. However, the focus in these papers is different, directed at the computation of statistical properties of star-graph spectra. There is no attempt in any of these papers to compute individual energy eigenvalues of quantum graphs exactly, explicitly via periodic-orbit expansions.

Because of the higher complexity of the spectrum of the three-pronged star graph, we have to discuss the rational case and the irrational case of the three-pronged star graph separately. In the rational case, the lengths of the edges of the three-pronged star graph are rationally related; in the irrational case, at least one pair of edges are irrationally related. Sections 2–6 explicitly assume the irrational case; the rational case is discussed in section 8.

This paper is structured in the following way. In section 2, we derive the spectral equation of the three-pronged star graph. In section 3, we study the organization of the spectral points of the three-pronged star graph. In particular, we show that the spectral points exhibit a lattice structure with only one spectral point per lattice cell. This global property of the spectrum is the key to the construction of explicit periodic-orbit formulae in section 6. In section 4, we

rederive the spectral equation using scattering quantization [1, 2, 14]. The scattering matrix S constructed for this purpose is the basis for the construction of the spectral staircase and the periodic-orbit formulae in section 6. In section 5, we state an explicit spectral formula that still contains an integral. In section 6, we perform this integral explicitly and arrive at an integral-free solution formula for the entire spectrum of the three-pronged star graph. In section 7, we investigate the convergence properties of our periodic-orbit expansions. The rational case is discussed in section 8. In some cases, the spectral points of the three-pronged star graph can be computed analytically by directly solving the spectral equation. Since the same roots may also be computed by using the periodic-orbit expansion formulae derived in section 6, we obtain exact sum rules for the periodic orbits of the three-pronged star graph and even some novel, arithmetic expansions of π^2. While up to and including section 8, for the purpose of definiteness, we assumed Dirichlet boundary conditions at the dead-end vertices, we show in section 9 that this assumption is not necessary and state explicitly a spectral formula that includes the case of Dirichlet boundary conditions and covers additional choices of boundary conditions. In section 10, we discuss our results. In section 11, we summarize our results and conclude this paper.

2. Spectral equation

We are looking for the bound states of the quantum particle on the graph. Denoting by m the mass of the particle and by E its energy,

$$k = \sqrt{\frac{2mE}{\hbar^2}} \tag{1}$$

is the wave number of the quantum particle on the graph. Since we are only interested in the bound states of the quantum graph, we assume, without restriction of generality, $k > 0$ throughout this paper. Referring to figure 2, we denote by $\psi_a(x_a)$, $\psi_b(x_b)$ and $\psi_c(x_c)$ the wavefunctions of the quantum particle on the edges a, b and c, respectively. Then, assuming Dirichlet boundary conditions at the vertices V_a, V_b and V_c requires that

$$\begin{aligned} &\psi_a(x_a) = A\sin[k(x_a - a)], \qquad \psi_b(x_b) = B\sin[k(x_b - b)], \\ &\psi_c(x_c) = C\sin[k(x_c - c)], \end{aligned} \tag{2}$$

where A, B and C are constants. Continuity of the wavefunction at the central vertex V_0 ($x_a = x_b = x_c = 0$) requires

$$A\sin(ka) = B\sin(kb) = C\sin(kc). \tag{3}$$

There are many ways to implement flux conservation at the central vertex V_0 [14]. A natural choice is to require that the sum of the incoming (outgoing) derivatives at V_0 be zero. In our case this results in

$$A\cos(ka) + B\cos(kb) + C\cos(kc) = 0. \tag{4}$$

In order to obtain a bound state of the quantum graph, (3) and (4) have to be fulfilled simultaneously. We consolidate conditions (3) and (4) into a single spectral equation whose roots are the spectrum of the quantum graph. To this end, we multiply the first term in (4) by $BC\sin(kb)\sin(kc)$, the second term in (4) by $AC\sin(ka)\sin(kc)$ and the third term in (4) by $AB\sin(ka)\sin(kb)$. Dividing the result by ABC and using appropriate trigonometric identities, we obtain the following spectral equation of the three-pronged star graph,

$$\cos(kL) - \tfrac{1}{3}[\cos(kL_1) + \cos(kL_2) + \cos(kL_3)] = 0, \tag{5}$$

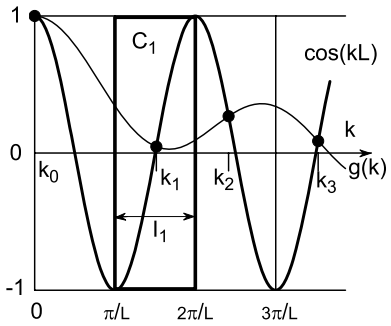

Figure 3. Organization of the spectrum of the three-pronged star graph. The spectral points $k_1, k_2, \ldots$, the abscissae of the intersections (full dots) of $\cos(kL)$ (heavy line) with $g(k)$ (thin line) are organized into root cells $C_n = I_n \times [-1, 1]$, $I_n = \{k : n\pi/L \leqslant k \leqslant (n+1)\pi/L\}$, $n = 1, 2, \ldots$, such that there is exactly one spectral point (intersection) in each root cell. As an example, we show root cell C_1 (framed rectangle) together with its associated root interval I_1 (double arrow). Parameters: $a = 1$, $b = 1/\sqrt{2}$, $c = 1/\pi$.

where

$$L = a + b + c, \qquad L_1 = |a + b - c|, \qquad L_2 = |a - b + c|,$$
$$L_3 = |a - b - c|. \tag{6}$$

The solutions k_n, $n = 1, 2, \ldots$ of (5) yield the quantum energy levels E_n of the three-pronged star graph according to

$$E_n = \frac{\hbar^2 k_n^2}{2m}, \tag{7}$$

where m is the mass of the quantum particle on the graph. Closed-form algebraic solutions of the spectral equation (5) can only be obtained in certain special cases, some of which are briefly discussed in section 8. In the irrational case, (5) cannot be solved algebraically in closed form. However, as shown in section 6, there is a way to obtain all solutions of (5) explicitly, and analytically, using exact periodic-orbit expansions.

3. Organization of the spectrum

Figure 3 shows the functions $\cos(kL)$ (heavy line) and

$$g(k) = \tfrac{1}{3}[\cos(L_1 k) + \cos(L_2 k) + \cos(L_3 k)] \tag{8}$$

(thin line) for $k > 0$. The intersections of these two functions are the solutions $k_1, k_2, \ldots$ of the spectral equation (5). We see that $\cos(kL)$ divides the k-axis naturally into intervals

$$I_n = \{k | n\pi/L \leqslant k \leqslant (n+1)\pi/L\}, \qquad n = 1, 2, 3, \ldots, \tag{9}$$

such that there appears to be exactly one root k_n in each of the intervals I_n. For this reason the intervals I_n are called root intervals [15]. In this section, we show that the organization of the spectrum into a regular lattice of root intervals with precisely one spectral point per root interval is rigorously true. This provides a global characterization of the spectrum, which is the key to obtaining exact periodic-orbit expansions for each of the solutions of (5).

First, we prove that in the irrational case, except for the trivial root $k_0 = 0$, none of the roots of (5) occur at integer multiples of π/L. According to figure 3 this would be the case only if $|g(N\pi/L)| = 1$, where N is an integer. But, according to (8) and because of $|\cos(L_j k)| \leqslant 1$,

this will happen only if $k = 0$ or $\cos(NL_j\pi/L) = \pm 1$, $j = 1, 2, 3$. Except for the trivial case $k = 0$ (no particle present), the latter condition implies that L_j/L, $j = 1, 2, 3$ are rational numbers, which, in turn, implies that a, b, c are rationally related. This, however, contradicts our assumption. Therefore, in the irrational case, none of the roots of (5) occur at multiples of π/L. Since the multiples of π/L are the borders of the root intervals (9), we have the result that, in the irrational case, and for all $k > 0$, the roots of (5) are located strictly *inside* of the root intervals (9).

Next, we prove that the spectrum of (5) is non-degenerate. We see this in the following way. Define the spectral function

$$f(k) = \cos(kL) - \tfrac{1}{3}[\cos(kL_1) + \cos(kL_2) + \cos(kL_3)]. \tag{10}$$

Then, the zeros of $f(k)$ are the zeros of the spectral equation (5). Let k^* be a degenerate zero of $f(k)$. Then

$$f(k^*) = 0, \qquad f'(k^*) = 0. \tag{11}$$

This implies the two equations

$$\cos(k^*L) = \tfrac{1}{3}[\cos(k^*L_1) + \cos(k^*L_2) + \cos(k^*L_3)] \tag{12}$$

and

$$\sin(k^*L) = \tfrac{1}{3}[\omega_1 \sin(k^*L_1) + \omega_2 \sin(k^*L_2) + \omega_3 \sin(k^*L_3)], \tag{13}$$

where

$$0 \leqslant \omega_j = \frac{L_j}{L} < 1, \qquad j = 1, 2, 3. \tag{14}$$

Adding the squares of (12) and (13) we obtain

$$\begin{aligned} 1 = \frac{1}{9}\Bigg\{ & \sum_{j=1}^{3}[\cos^2(k^*L_j) + \omega_j^2 \sin^2(k^*L_j)] \\ & + \sum_{l\neq m=1}^{3} [\cos(k^*L_l)\cos(k^*L_m) + \omega_l\omega_m \sin(k^*L_l)\sin(k^*L_m)]\Bigg\} \\ \leqslant \frac{1}{9}\sum_{j=1}^{3} & \left|\cos^2(k^*L_j) + \omega_j^2 \sin^2(k^*L_j)\right| \\ & + \frac{1}{9}\sum_{l\neq m=1}^{3} |\cos(k^*L_l)\cos(k^*L_m) + \omega_l\omega_m \sin(k^*L_l)\sin(k^*L_m)| \\ < 1. & \end{aligned} \tag{15}$$

This is so since, according to (14), ω_j, $j = 1, 2, 3$ are strictly smaller than 1, and, since L_l is irrationally related to L_m for $l \neq m$, at most two of the sine functions in (15) may be zero. We obtain a contradiction, which proves that degenerate zeros are impossible. Therefore, in the irrational case, the spectrum of the three-pronged star graph is non-degenerate.

We call the rectangles $C_n = I_n \times [-1, +1]$ in figure 3 the root cells of the spectrum. Figure 3 shows that $\cos(kL)$ divides each root cell into two equal parts with $\cos(kL)$ representing the border line between these two parts. Since $g(k)$ is a continuous function that has to traverse both parts of a root cell as a function of k, and since $|g(k)| \leqslant 1$ for all $k > 0$, there is at least one intersection of $g(k)$ with $\cos(kL)$ in each root cell. This means that there is at least one solution of (5) in each root interval I_n. We now show that there cannot be any other.

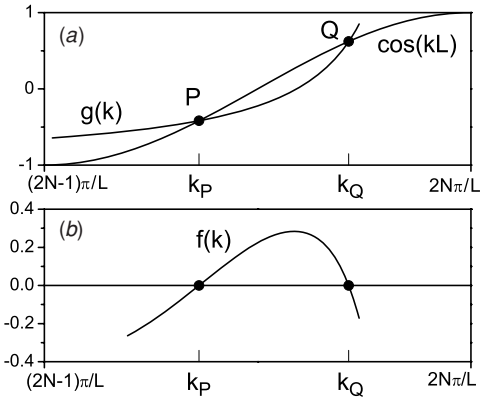

Figure 4. Hypothetical situation of two intersections in root cell C_{2N-1}. (*a*) $g(k)$ intersects $\cos(kL)$ in two points, P and Q (dots), with the associated k values k_P and k_Q, respectively. (*b*) Behavior of the spectral function $f(k)$ in the vicinity of k_P and k_Q, the abscissae of the two (hypothetical) intersections P and Q, respectively.

Let us focus first on the odd-numbered root cells C_{2n-1}, $n = 1, 2, \ldots$, in particular on root cell C_{2N-1} as a representative. We already proved that there is at least one spectral point in each root cell, i.e., there is at least one intersection of $g(k)$ with $\cos(kL)$ in C_{2N-1}. As shown in figure 4(*a*) we denote by P, with the associated k value k_P, the intersection with the smallest k value in C_{2N-1}. Let us now assume that there is a second intersection, Q, with the associated k value k_Q, in C_{2N-1} (see figure 4(*a*)). Since we already proved that all roots of $f(k)$ are simple and occur strictly inside of the root intervals, and since we assumed that k_P is the smallest zero in C_{2N-1}, we have

$$(2N-1)\pi/L < k_P < k_Q < 2N\pi/L. \tag{16}$$

As shown in figure 4(*a*), $\cos(kL)$ starts at -1 in an odd-numbered root cell. Since we already proved that $|g(k)| \leqslant 1$ for all $k > 0$, $f(k)$, as defined in (10), is negative for $k < k_P$ and positive for $k > k_P$ (see figure 4(*b*)) in the immediate vicinity of k_P. Since there are no roots between k_P and k_Q (both roots are simple, and by assumption k_P is the first and k_Q is the second root), $f(k)$ is positive for $k < k_Q$ and negative for $k > k_Q$ as shown in figure 4(*b*) in the immediate vicinity of k_Q. Therefore, the derivative

$$f'(k_Q) = \lim_{h\to 0}[f(k_Q + h) - f(k_Q - h)]/(2h), \tag{17}$$

as the limit of a strictly negative quantity, is either zero or negative. Since we already showed that all roots of $f(k)$ are simple (i.e. $f'(k^*) \neq 0$ for all spectral points k^*), $f'(k_Q)$ cannot be zero. Therefore,

$$f'(k_Q) < 0. \tag{18}$$

This, however, implies that

$$g'(k_Q) > -L\sin(k_Q L) > 0. \tag{19}$$

At Q, with the associated spectral point k_Q, we also have

$$\tfrac{1}{3}[\cos(L_1 k_Q) + \cos(L_2 k_Q) + \cos(L_3 k_Q)] = \cos(L k_Q). \tag{20}$$

Squaring (19) and (20) and adding their left- and right-hand sides, respectively, leads to the same equations, and ensuing contradiction, as established in (15). This shows that a second

intersection Q cannot exist in odd-numbered root cells. It is straightforward to adapt this argument for the even-numbered root cells (in which $\cos(kL)$ is monotonically decreasing), which shows that additional intersections Q are also not allowed in even-numbered root cells. Thus, in summary, we have shown that there exists exactly one root (i.e. the spectral point) per root interval.

The property of exactly one root per root interval suggests the following definition, which will be useful in later sections. Since we showed that (in the irrational case) no roots occur on the boundaries of the root intervals I_n, and since there is only a single root per root interval, the boundaries $n\pi/L$ of the root intervals separate the roots of (5) from each other. Therefore, we call the boundaries of the root intervals the root separators [16] and define the left and right root separators of the spectral point k_n in the following way:

$$k_n^{(-)} = n\pi/L < k_n < k_n^{(+)} = (n+1)\pi/L, \quad n = 1, 2, \ldots. \tag{21}$$

The root separators will play an important role in sections 5 and 6.

The lattice organization of the roots of (5), with precisely one spectral point per root interval, implies that the average density of states of the three-pronged star graph is

$$\bar{\rho}(k) = \frac{\text{one root}}{\text{root interval}} = \frac{1}{\pi/L} = \frac{L}{\pi}. \tag{22}$$

This result is known and applies generally to all (non-dressed) quantum graphs [1–4]. The point of presenting it here is to show that (22) (i) may be derived independently in an elementary way via the root separators and (ii) is consistent with the known result.

There is another way of obtaining root separators sometimes used in the literature to derive statistical properties of quantum graph spectra [11–13]. Defining $l_1 = a, l_2 = b, l_3 = c$ and dividing (4) by (3) results in

$$\sum_{b=1}^{3} \cot(kl_b) = 0, \tag{23}$$

which can immediately be generalized to $\sum_{b=1}^{B} \cot(kl_b) = 0$, valid for any star graph with B bonds and Dirichlet boundary conditions [11–13]. A separating set of the spectral equation (23) is $A' = \{j\pi/l_b, j = 1, 2, \ldots, b = 1, \ldots, B\}$ [11–13]. This set is an unordered, interlacing set of B incommensurate subsets. Because it is not ordered, it is not known which spectral point k_n is located between which root separators of A'. Thus, the set A' is useless for isolating the nth spectral point, and thus is useless for computing explicit spectral eigenvalues.

4. Scattering quantization

Using flux conservation and the continuity of the wavefunction is one way of deriving the spectral equation for the three-pronged star graph. Another way is via scattering quantization [1, 2, 14]. This method is better suited for our purpose of deriving explicit spectral formulae in sections 5 and 6. Thus, the purpose of this section is to derive the graph scattering matrix S, prove some useful properties of S and, eventually, rederive the spectral equation on the basis of S.

The arrows in figure 5 indicate the six different ways, called channels, in which quantum flux can move on a three-pronged star graph. The channels are numbered sequentially from 1 to 6; in figure 5 the channel numbers appear next to the corresponding channel arrows. In channel 1, e.g., as indicated by the corresponding arrow, flux moves in the direction from V_0 to V_a.

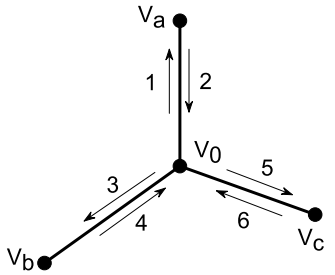

Figure 5. Channel assignment for the three-pronged star graph.

The 6×6 graph scattering matrix $S(k)$ describes the redistribution of flux on the graph following one scattering event at energy $E = \hbar^2 k^2/(2m)$. Starting with unit flux in channel l, the matrix element S_{ml} is the amplitude of flux scattered from channel l into channel m. Thus the index l refers to the input channels of $S(k)$; the index m refers to the output channels. Apparently, because of flux conservation,

$$\sum_{m=1}^{6} |S_{ml}(k)|^2 = 1, \qquad l = 1, \ldots, 6. \tag{24}$$

In fact, since no flux is ever lost on the graph, $S(k)$ is unitary, i.e.

$$S^\dagger(k) S(k) = \mathbf{1}, \tag{25}$$

where $\mathbf{1}$ is the 6×6 unit matrix.

To construct the S matrix explicitly, consider the following example. A quantum particle in channel 1, described by the wavefunction $\exp(\mathrm{i}kx_a)$, moves from V_0 to the dead-end vertex V_a. On its journey to V_a it picks up a phase $\exp(\mathrm{i}ka)$. Scattering off the dead-end vertex V_a, which, for Dirichlet boundary conditions, is equivalent to a 'hard wall', it picks up an additional phase factor -1. Immediately after scattering off V_a, the particle is ready to enter channel 2, i.e. it will next travel from V_a to V_0. Apparently, when starting in channel 1 and allowing for only one scattering event, channel 2 is the only exit channel the quantum particle can scatter into. Therefore,

$$S_{21} = -\mathrm{e}^{\mathrm{i}ka}, \qquad S_{m1} = 0, \quad m \neq 2. \tag{26}$$

This is the first column of the S matrix.

If we start in channel 2, we pick up the phase $\exp(\mathrm{i}ka)$ traveling from V_a to V_0. At V_0 we may transmit into channels 3 and 5 with transmission amplitudes t_3 and t_5, respectively, or we may reflect off V_0 and enter channel 1 with reflection amplitude r. The channel wavefunctions in channels 3 and 5 are $t_3 \exp(\mathrm{i}kx_b)$ and $t_5 \exp(\mathrm{i}kx_c)$, respectively. Continuity of the scattering wavefunction at V_0 ($x_b = x_c = 0$) requires $t_3 = t_5 = t$. Therefore,

$$\begin{aligned} &S_{12} = r\,\mathrm{e}^{\mathrm{i}ka}, \qquad &&S_{22} = 0, \qquad &&S_{32} = t\,\mathrm{e}^{\mathrm{i}ka}, \\ &S_{42} = 0, \qquad &&S_{52} = t\,\mathrm{e}^{\mathrm{i}ka}, \qquad &&S_{62} = 0. \end{aligned} \tag{27}$$

This is the second column of the S matrix. Similar reasoning, considering the graph scattering problem with initial unit flux in channels $3, \ldots, 6$, establishes that

$$S(k) = \begin{pmatrix} 0 & r\,\mathrm{e}^{\mathrm{i}ka} & 0 & t\,\mathrm{e}^{\mathrm{i}kb} & 0 & t\,\mathrm{e}^{\mathrm{i}kc} \\ -\mathrm{e}^{\mathrm{i}ka} & 0 & 0 & 0 & 0 & 0 \\ 0 & t\,\mathrm{e}^{\mathrm{i}ka} & 0 & r\,\mathrm{e}^{\mathrm{i}kb} & 0 & t\,\mathrm{e}^{\mathrm{i}kc} \\ 0 & 0 & -\mathrm{e}^{\mathrm{i}kb} & 0 & 0 & 0 \\ 0 & t\,\mathrm{e}^{\mathrm{i}ka} & 0 & t\,\mathrm{e}^{\mathrm{i}kb} & 0 & r\,\mathrm{e}^{\mathrm{i}kc} \\ 0 & 0 & 0 & 0 & -\mathrm{e}^{\mathrm{i}kc} & 0 \end{pmatrix}. \tag{28}$$

To derive the numerical values of the reflection and transmission amplitudes r and t in (28), we need to solve the graph scattering problem at the central vertex V_0. To do this, consider, without restriction of generality, the scattering problem where the quantum particle is initially in channel 2. In this case the wavefunction on edge a is $\exp(-\mathrm{i}kx_a) + r\exp(\mathrm{i}kx_a)$, while the wavefunctions on edges b and c are $t\exp(\mathrm{i}kx_b)$ and $t\exp(\mathrm{i}kx_c)$, respectively. Continuity of the wavefunction at V_0 ($x_a = x_b = x_c = 0$) requires

$$1 + r = t. \tag{29}$$

Flux conservation at V_0 requires

$$-1 + r + 2t = 0. \tag{30}$$

Solving the linear system of equations (29) and (30), we obtain

$$r = -\tfrac{1}{3}, \qquad t = \tfrac{2}{3}. \tag{31}$$

All odd powers of $S(k)$ have the structure (28). Therefore, it follows immediately that

$$\mathrm{Tr}[S^{2N+1}(k)] = 0, \qquad N = 0, 1, \ldots, \tag{32}$$

i.e. the trace of all odd powers of S is zero.

Next, we use the graph scattering matrix $S(k)$ to rederive the spectral equation for the three-pronged star graph. We reason in the following way. Since $S(k)$ describes the redistribution of flux on the graph, we obtain a stationary state $|\psi\rangle$ of the quantum graph if $|\psi\rangle$ is invariant under application of $S(k)$. This means that

$$S(k)|\psi\rangle = |\psi\rangle. \tag{33}$$

For a non-trivial solution $|\psi\rangle$ of this eigenvalue equation, we need to require that

$$\det[S(k) - \mathbf{1}] = 0. \tag{34}$$

This gives us a condition on the allowed values of k, which are the spectral points $k_1, k_2, \ldots$ of the three-pronged star graph. But this, in turn, means that $\det[S(k) - \mathbf{1}]$ must have the same zeros as the spectral function $f(k)$ defined in (10). Indeed, an explicit calculation shows that

$$\det[S(k) - \mathbf{1}] = 2\,\mathrm{e}^{\mathrm{i}kL} f(k). \tag{35}$$

Thus, as expected, $\det[S(k) - \mathbf{1}]$ has the same zeros as the spectral function $f(k)$. We will use this fact as the starting point for the derivation of the spectral staircase and the explicit spectral formulae of the three-pronged star graph in the following sections.

5. Spectral points: explicit solution via reduction to quadratures

The purpose of this section is to solve the spectral equation (5) analytically. In preparation for obtaining the explicit solution formula, we define

$$\Theta_{2\pi}(x) = \sum_{m=-\infty}^{\infty} \theta(x - 2\pi m), \tag{36}$$

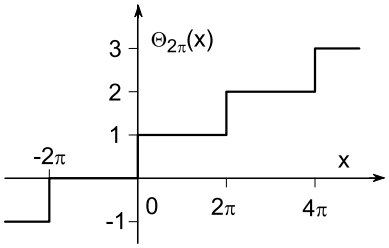

Figure 6. Graph of $\Theta_{2\pi}(x)$.

where

$$\theta(x) = \begin{cases} 0, & \text{for} \quad x < 0, \\ 1/2, & \text{for} \quad x = 0, \\ 1, & \text{for} \quad x > 0 \end{cases} \tag{37}$$

is Heaviside's step function. A plot of $\Theta_{2\pi}(x)$ is shown in figure 6. It is a staircase function with unit step height and step width 2π. $\Theta_{2\pi}(x)$ is normalized such that $\Theta_{2\pi}(0) = 1/2$. This way we have $\Theta_{2\pi}(x) = \theta(x)$ in $-2\pi < x < 2\pi$. A Fourier series representation of $\Theta_{2\pi}(x)$ is

$$\Theta_{2\pi}(x) = \frac{1}{2} + \frac{x}{2\pi} + \frac{1}{\pi}\sum_{m=1}^{\infty}\frac{\sin(mx)}{m}. \tag{38}$$

Next, we define the spectral staircase of the three-pronged star graph according to

$$N(k) = \sum_{n=1}^{\infty}\theta(k - k_n). \tag{39}$$

Note that we do not include the trivial zero $k_0 = 0$ in the definition of the spectral staircase since $k_0 = 0$ corresponds to the graph without a quantum particle on it. Thus, $N(k)$ is zero until it hits the first non-trivial spectral point $k_1 > 0$.

Concluding the preliminaries, consider the spectral staircase (39) in the interval $k_n^{(-)} < k < k_n^{(+)}$, where $k_n^{(-)}$ and $k_n^{(+)}$ are the root separators defined in (21). As shown in figure 7, the staircase function equals $n - 1$ for $k_n^{(-)} < k < k_n$, jumps by one unit at $k = k_n$ and equals n for $k_n < k < k_n^{(+)}$. Therefore

$$\int_{k_n^{(-)}}^{k_n^{(+)}} N(k)\,\mathrm{d}k = (n-1)\left[k_n - k_n^{(-)}\right] + n\left[k_n^{(+)} - k_n\right]. \tag{40}$$

Solving this equation for k_n and using the expressions (21) for $k_n^{(-)}$ and $k_n^{(+)}$, we obtain

$$k_n = \frac{2n\pi}{L} - \int_{n\pi/L}^{(n+1)\pi/L} N(k)\,\mathrm{d}k. \tag{41}$$

This is an explicit formula for k_n as soon as we have an explicit expression for $N(k)$. Therefore, in the remainder of this section, we will derive this expression.

We start with the spectral equation in the form (34). Since $S(k)$ is unitary, it can be diagonalized. Its eigenvalues are $\lambda_j(k) = \exp[\mathrm{i}\sigma_j(k)]$, $j = 1, \ldots, 6$, where $\sigma_j(k)$, called S-matrix eigenphases, are real for all k. Since the spectral equation

$$\det[S(k) - \mathbf{1}] = \prod_{j=1}^{6}[\mathrm{e}^{\mathrm{i}\sigma_j(k)} - 1] = 0 \tag{42}$$

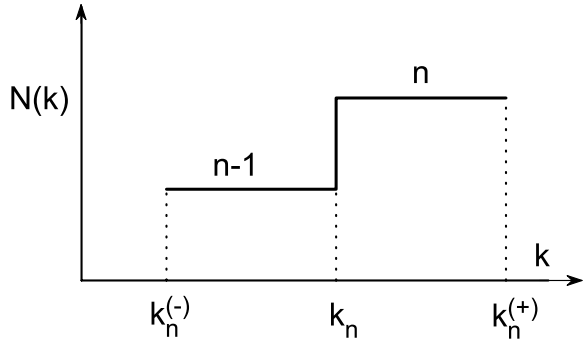

Figure 7. Staircase function $N(k)$ in the vicinity of the spectral point k_n.

is satisfied as soon as any one of the $\sigma_j(k)$ is an integer multiple of 2π, we may write the spectral staircase (39) in the form

$$N(k) = N_0 + \sum_{j=1}^{6} \Theta_{2\pi}[\sigma_j(k)], \tag{43}$$

where N_0 is a constant. We note that since for $k > 0$ the zeros of (5) (or, equivalently, (34)) are simple, no two $\sigma_j(k)$ are ever simultaneously integer multiples of 2π for $k > 0$.

Since the trace of a matrix is invariant under unitary transformations, the trace of S is the same as the trace of the diagonalized S. Using this fact, we obtain

$$\mathrm{Im}\,\mathrm{Tr}[S^n(k)] = \mathrm{Im} \sum_{j=1}^{6} \mathrm{e}^{\mathrm{i}n\sigma_j(k)} = \sum_{j=1}^{6} \sin[n\sigma_j(k)]. \tag{44}$$

With this result and using the Fourier representation (38) of $\Theta_{2\pi}$, we may write (43) in the form

$$\begin{aligned} N(k) &= N_0 + \sum_{j=1}^{6} \left\{ \frac{1}{2} + \frac{\sigma_j(k)}{2\pi} + \frac{1}{\pi} \sum_{m=1}^{\infty} \frac{\sin[m\sigma_j(k)]}{m} \right\} \\ &= N_0 + 3 + \frac{1}{2\pi} \sum_{j=1}^{6} \sigma_j(k) + \frac{1}{\pi}\,\mathrm{Im}\,\mathrm{Tr} \sum_{m=1}^{\infty} \frac{1}{m} S^m(k). \end{aligned} \tag{45}$$

We evaluate the sum over the S-matrix eigenphases in the following way. First, we note that

$$\det[S(k)] = \prod_{j=1}^{6} \exp[\mathrm{i}\sigma_j(k)] = \exp\left[\mathrm{i} \sum_{j=1}^{6} \sigma_j(k) \right]. \tag{46}$$

Then, the direct algebraic calculation of $\det[S(k)]$, using its explicit representation (28), yields

$$\det[S(k)] = \exp(2\,\mathrm{i}kL). \tag{47}$$

Therefore,

$$\sum_{j=1}^{6} \sigma_j(k) = 2kL. \tag{48}$$

Inserting this equation into (45) we obtain

$$N(k) = N_0 + 3 + \left(\frac{kL}{\pi}\right) + \frac{1}{2\pi}\,\mathrm{Im\,Tr}\sum_{m=1}^{\infty}\frac{1}{m}S^{2m}(k), \tag{49}$$

where we also used the fact (see (32)) that the traces of all odd powers of S are zero.

We are now ready to determine the constant N_0. According to (39) the spectral staircase $N(k)$ is zero in the interval $0 < k < \epsilon$, where $0 < \epsilon \ll k_1$. The constant N_0 has to be determined to reflect this fact. We derive N_0 from (43), which requires knowledge of the eigenphases $\sigma_j(k)$ for small k. For $k = 0$ it is straightforward to diagonalize $S(k)$ defined in (28) analytically. We obtain the eigenvalues $\lambda_1(0) = 1, \lambda_2(0) = 1$, $\lambda_3(0) = -1, \lambda_4(0) = -1, \lambda_5(0) = -i$ and $\lambda_6(0) = i$. Since $\lambda = \exp(\mathrm{i}\sigma)$, and taking (48) into account, which implies $\sum_{j=1}^{6}\sigma_j(k=0) = 0$, we obtain the eigenphases $\sigma_1(k=0) = 0, \sigma_2(k=0) = 0, \sigma_3(k=0) = -\pi, \sigma_4(k=0) = \pi, \sigma_5(k=0) = -\pi/2$ and $\sigma_6(k=0) = \pi/2$. Other phase conventions may be used. They will not change the following results as long as they are consistent with (48). Since the S-matrix eigenphases are continuous and monotonically increasing functions of k [1, 2, 14], we now obtain (see figure 6) $\theta_{2\pi}(\sigma_1(\epsilon)) = 1, \theta_{2\pi}(\sigma_2(\epsilon)) = 1, \theta_{2\pi}(\sigma_3(\epsilon)) = 0, \theta_{2\pi}(\sigma_4(\epsilon)) = 1, \theta_{2\pi}(\sigma_5(\epsilon)) = 0$ and $\theta_{2\pi}(\sigma_6(\epsilon)) = 1$. This means that $\sum_{j=1}^{6}\theta_{2\pi}(\sigma_j(\epsilon)) = 4$ and therefore, since $N(\epsilon) = 0$, $N_0 = -4$. With this result we arrive at the explicit expression

$$N(k) = -1 + \left(\frac{kL}{\pi}\right) + \frac{1}{2\pi}\,\mathrm{Im\,Tr}\sum_{m=1}^{\infty}\frac{1}{m}S^{2m}(k). \tag{50}$$

This expression for the spectral staircase function is consistent with the results presented in [4]. We now use (50) in (41) to arrive at the explicit formula

$$k_n = \frac{\pi}{L}\left(n + \frac{1}{2}\right) - \frac{1}{2\pi}\,\mathrm{Im\,Tr}\sum_{m=1}^{\infty}\frac{1}{m}\int_{n\pi/L}^{(n+1)\pi/L} S^{2m}(k)\,\mathrm{d}k \tag{51}$$

for the spectral points of the three-pronged star graph. This result still contains integrals (quadratures) to perform. An integral-free expression in terms of periodic orbits is derived in the following section.

6. Exact periodic-orbit expansions

Since r and t are constants, the matrix elements of the S matrix (28) are simple exponential functions of k, and powers of the S matrix are sums of exponential functions. Therefore, there is no problem to perform the integrals in (51) analytically, term by term. However, if we aim for explicit, analytical formulae for these integrals, we need an efficient way of book keeping, i.e., we need a way of writing down the sums of exponential functions generated by the powers of the S matrix in (51). Periodic-orbit theory provides the book keeping we are looking for. The key is to relate the trace of $S^{2m}(k)$ to periodic orbits on the graph. To get a feeling of how this works, let us look at the first term of the sum in (51) which requires us to compute

$$\mathrm{Tr}[S^2(k)] = 2[-r\,\mathrm{e}^{2\,\mathrm{i}ka} - r\,\mathrm{e}^{2\,\mathrm{i}kb} - r\,\mathrm{e}^{2\,\mathrm{i}kc}]. \tag{52}$$

We interpret this result in terms of periodic orbits in the following way. The first term inside the brackets in (52) corresponds to a quantum particle starting somewhere on edge a, heading toward the central vertex, reflecting off the central vertex V_0 to return to edge a, reflecting off the dead-end vertex V_a and returning to its starting point on a. This way the particle has traversed the shortest possible periodic orbit on edge a. Reflecting off the central vertex V_0,

the particle acquires the phase factor r, and reflecting off the dead-end vertex V_a, it acquires the phase factor -1. This accounts for the factor $-r$ in front of the first exponential function inside the brackets in (52). The argument of this exponential function is i times the total classical action (in units of $\hbar$), $\int k\,\mathrm{d}x = 2ka$, accumulated by the particle on its round trip traversing the periodic orbit. A similar interpretation applies to the second and third terms in (52). The global factor 2 multiplying the brackets in (52) arises because of the time-reversal invariance of the dynamics of the quantum particle on the graph. Equivalently, the factor 2 may also be seen as arising from the fact that the particle may traverse a periodic orbit with its initial momentum directed away from the central vertex or directed toward the central vertex without changing the phase factors or the exponential factors in (52). Similar reasoning may be applied to higher powers of S. We obtain

$$\mathrm{Tr}\, S^{2m}(k) = 2\sum_p \sum_{\nu l_p = m} l_p [(-1)^{l_p} r^{\alpha_p} t^{\beta_p}]^\nu \, \mathrm{e}^{\mathrm{i}\nu k L_p}. \tag{53}$$

The different symbols in (53) have the following meanings. The first sum in (53) is over all primitive periodic orbits p of the three-pronged star graph. A primitive periodic orbit is one that cannot be interpreted in terms of multiple traversals of a shorter periodic orbit. The symbol l_p denotes the total number of bounces of p off the dead-end vertices of the graph. The symbol ν is the repetition index. It denotes the number of times the primitive periodic orbit is traversed. According to the restriction on the second sum in (53), $\nu l_p = m$, not all periodic orbits enter into the sum for given m. Only those periodic orbits enter whose 'length' l_p in terms of number of bounces off the dead-end vertices divides m. The symbols α_p and β_p in (53) denote the number of reflections off and transmissions through the central vertex V_0, respectively. The total physical length of the primitive periodic orbit p in terms of the edge lengths a, b and c is denoted by L_p in (53).

With (53) we are now ready to perform the integrals in (51), obtaining

$$k_n = \frac{\pi}{L}\left(n+\frac{1}{2}\right) - \frac{2}{\pi}\sum_{m=1}^{\infty}\sum_p \sum_{\nu l_p = m} \frac{1}{\nu^2 L_p}[(-1)^{l_p} r^{\alpha_p} t^{\beta_p}]^\nu \times \sin\left[\nu\pi\left(n+\frac{1}{2}\right)\left(\frac{L_p}{L}\right)\right]\sin\left[\nu\pi\left(\frac{L_p}{2L}\right)\right]. \tag{54}$$

With this equation we have arrived at the central result of this paper: an explicit, exact, integral-free periodic-orbit expansion of the spectral points of the three-pronged star graph.

7. Convergence

In order to assess the speed of convergence of the explicit spectral formulae (51) and (54), we define $k_n^{(M)}$ as an approximation to the exact spectral point k_n by including only the first M terms in the m sums of (51) (or, equivalently, (54)). Figure 8 shows

$$\Delta_1^{(M)} = \left|k_1^{(M)} - k_1\right| \tag{55}$$

(ragged line) as a function of M computed via formula (51). We see that $\Delta_1^{(M)}$ converges to zero, i.e., (51) converges to the exact spectral point k_1. Also shown in figure 8 is the function $0.1/M^2$ (straight line) to guide the eye. We see that on average $\Delta_1^{(M)}$ is close to $0.1/M^2$, i.e. $\Delta_1^{(M)} \sim 1/M^2$. Since (54) is equivalent to (51), (54) has the same convergence behavior in M after summation over the periodic orbits is performed for each m term in (54). We checked that qualitatively the same behavior, including the $\sim 1/M^2$ convergence, is observed for $\Delta_n^{(M)}$, $n = 10, 100, 1000$.

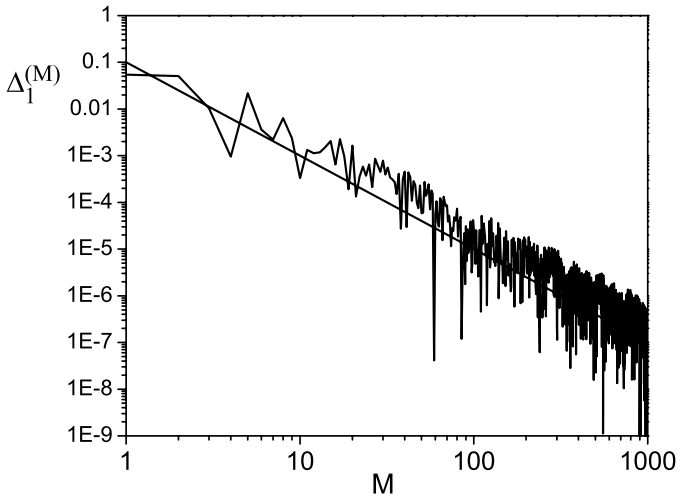

Figure 8. Convergence of $k_1^{(M)}$ as a function of the number M of S-matrix terms included in the m sum of (51). The ragged line is the absolute value $\Delta_1^{(M)} = |k_1^{(M)} - k_1|$ of the difference between the truncated value $k_1^{(M)}$ and the exact value k_1. We see that $\Delta_1^{(M)} \to 0$, i.e., $k_1^{(M)} \to k_1$ for $M \to \infty$. A straight line, $0.1/M^2$, is drawn to guide the eye and to corroborate the $\sim 1/M^2$ convergence of $\Delta_1^{(M)}$. Parameters: $a = 1, b = 1/\sqrt{2}, c = 1/\pi$.

The number of periodic orbits to be summed for given m is [17]

$$\mathcal{N}_m = \frac{1}{m} \sum_{d|m} \phi(d) 3^{m/d}, \tag{56}$$

where the sum is over all divisors of m (including $d = 1$ and $d = m$) and ϕ is Euler's totient function. As an order-of-magnitude estimate we approximate $\mathcal{N}_m$ by the first term ($d = 1$) in (56) and obtain $\mathcal{N}_m \approx 3^m/m$. Therefore, the total number of periodic orbits included up to $m = M$ is

$$\mathcal{N}(M) = \sum_{m=1}^{M} \mathcal{N}_m \approx \sum_{m=1}^{M} 3^m/m \approx 3^{M+1}/(2M). \tag{57}$$

Solving this equation for M and keeping only terms of leading order in M, we obtain $M \approx \ln[\mathcal{N}(M)]/\ln(3)$ or

$$\Delta_1^{(M)} \sim 1/\{\ln[\mathcal{N}(M)]\}^2. \tag{58}$$

From (58) we see that the periodic-orbit expansion (54) converges extremely slowly in the number of periodic orbits $\mathcal{N}(M)$. On the other hand, we see from figure 8 that even for small M, i.e. only a few periodic orbits are included, the accuracy is already very good. Therefore, concerning our three-pronged star graph, we obtain the following recommendation: periodic-orbit expansions are the tool of choice if modest, but uniform accuracy is required over the entire spectral range from $k = 0$ to $k = \infty$. For $M = 3$, for instance, 20 periodic orbits are included in (54). We checked that in this case $\left|k_n^{(3)} - k_n\right| < 0.135$ for $1 \leqslant n \leqslant 10^5$. For $M = 4$, corresponding to 44 included orbits, we obtain $\left|k_n^{(4)} - k_n\right| < 0.097$ for $1 \leqslant n \leqslant 10^5$. Thus, compared with the length $\pi/L = \pi/(1 + 1/\sqrt{2} + 1/\pi) \approx \pi/2$ of the root interval, the relative error is uniformly smaller than 10% if the first 20 periodic orbits are included; it is smaller than 7% if the first 44 periodic orbits are included. If high accuracy is required,

periodic-orbit expansions will fail. For example, as shown in figure 8, for $\Delta_1^{(M)} \sim 10^{-7}$ we need $M \sim 1000$, which corresponds to $\mathcal{N}(M) \sim 3^{1000} \approx 10^{477}$ periodic orbits. Therefore, in cases where the aim is not a deeper analytical understanding of the global properties of the spectrum, but high-accuracy results of individual spectral points, numerical methods are recommended.

8. Rational case

Up until now, we focused our discussion of the spectrum on the irrational case in which none of the edge lengths a, b and c of the three-pronged star graph are rationally related. We did this to avoid complications in the discussion. For instance, only in the irrational case do we arrive at the spectral equation (5) by equivalence transformations, while these transformations may result in 'illegal' operations (for instance, division by zero) in the rational case. However, it turns out that (5) is valid in the rational case, too. This can be understood on the basis of a 'perturbation argument'. Perturbing away from rational, we are in the irrational case where (5) applies. Since the roots for the rational case should go smoothly into the roots for the irrational case when we approximate the rational case with a sequence of irrational numbers, the same spectral equation is expected to hold.

A similar problem exists with the root separators. In the rational case, zeros of (5) may lie squarely on the root separators. Also, the spectrum may no longer be simple and energy levels may be up to two-fold degenerate. Even more: degenerate zeros of (5) may lie on the root separators. All these observations may produce considerable concern until we realize that (i) the final result (54) is entirely based on the S matrix, which applies irrespective of whether we are in the rational or in the irrational case, (ii) the possibility of degenerate roots is automatically included and properly accounted for by the staircase function (50) and (iii) the general formula (41) works even if a single or a double root coincides with a root separator. All this taken together means that the periodic-orbit expansion (54) works even in the rational case.

The rational case does not only offer difficulties. It also offers something new. Since some star graphs with rationally related edge lengths are algebraically solvable, the spectrum of the three-pronged star graph may be expressed in two ways, algebraically and with the help of the periodic-orbit expansion (54). This results in sum rules for the periodic orbits on the three-pronged star graph. For $a = b = c$, e.g., we can compute all the powers of S analytically. We obtain

$$\begin{aligned} \operatorname{Tr} S^{4m+2}(k) &= 2\,\mathrm{e}^{(4m+2)\,\mathrm{i}ka}, \qquad m = 0, 1, 2, \ldots, \\ \operatorname{Tr} S^{4m}(k) &= 6\,\mathrm{e}^{4m\,\mathrm{i}ka}, \qquad m = 1, 2, \ldots, \end{aligned} \tag{59}$$

from which we obtain the periodic-orbit sum rules

$$\sum_p \sum_{vl_p=m} l_p \left[(-1)^{l_p} \left(-\frac{1}{3}\right)^{\alpha_p} \left(\frac{2}{3}\right)^{\beta_p} \right]^v = \begin{cases} 1, & \text{for} \quad m = 1, 3, 5, \ldots, \\ 3, & \text{for} \quad m = 2, 4, 6, \ldots. \end{cases} \tag{60}$$

Moreover, for $a = b = c$, the first non-trivial solution of (5) is $k_1 = \pi/(2a)$. Since, for $a = b = c$, we know all the powers of S analytically, this root can also be computed via (51). Equating both results and solving for π^2, we obtain

$$\pi^2 = \frac{1}{\frac{1}{2}(\delta_2 - \delta_1) - \frac{3}{4}(\delta_2^2 - \delta_1^2)} \sum_{m=1}^{\infty} \frac{1 + 2(-1)^m}{m^2} [\cos(m\pi\delta_1) - \cos(m\pi\delta_2)], \tag{61}$$

where we chose the root separators

$$k_1^{(-)} = \frac{\pi}{2a}(1-\delta_1), \qquad k_1^{(+)} = \frac{\pi}{2a}(1+\delta_2), \qquad 0 < \delta_1, \quad \delta_2 \leqslant 1. \tag{62}$$

Since π occurs in the arguments of the cosine functions on the right-hand side of (61), (61) does not appear to be an explicit expansion of π^2. However, if we choose δ_1 and δ_2 rational, such that the cosines in (61) can be evaluated algebraically, we obtain a host of novel, arithmetic series expansions for π^2. The well-known formula

$$\pi^2 = 8\sum_{m=0}^{\infty}\frac{1}{(2m+1)^2} \tag{63}$$

is included in (61) for the choice $\delta_1 = 1$, $\delta_2 = 1/2$.

9. Alternative boundary conditions

Up to now, we assumed Dirichlet boundary conditions at the dead-end vertices V_a, V_b and V_c. However, we may specify any combination of Dirichlet or Neumann boundary conditions at the vertices and our methods still work. Let us define

$$\varphi = \begin{cases} -1, & \text{for Dirichlet boundary conditions,} \\ +1, & \text{for Neumann boundary conditions,} \end{cases} \tag{64}$$

and let $\varphi_a, \varphi_b, \varphi_c$ denote the phases corresponding to the boundary conditions chosen at V_a, V_b and V_c, respectively. Then, the S matrix is

$$S(k) = \begin{pmatrix} 0 & r\,\mathrm{e}^{\mathrm{i}ka} & 0 & t\,\mathrm{e}^{\mathrm{i}kb} & 0 & t\,\mathrm{e}^{\mathrm{i}kc} \\ \varphi_a\,\mathrm{e}^{\mathrm{i}ka} & 0 & 0 & 0 & 0 & 0 \\ 0 & t\,\mathrm{e}^{\mathrm{i}ka} & 0 & r\,\mathrm{e}^{\mathrm{i}kb} & 0 & t\,\mathrm{e}^{\mathrm{i}kc} \\ 0 & 0 & \varphi_b\,\mathrm{e}^{\mathrm{i}kb} & 0 & 0 & 0 \\ 0 & t\,\mathrm{e}^{\mathrm{i}ka} & 0 & t\,\mathrm{e}^{\mathrm{i}kb} & 0 & r\,\mathrm{e}^{\mathrm{i}kc} \\ 0 & 0 & 0 & 0 & \varphi_c\,\mathrm{e}^{\mathrm{i}kc} & 0 \end{pmatrix}. \tag{65}$$

We see that, except for the phase factors, the S matrix (65) is the same as the S matrix (28). This means that all derivation steps that lead to the periodic-orbit expansions of the spectral points remain valid if φ_a, φ_b and φ_c are properly accounted for. We obtain

$$k_n = \frac{\pi}{L}\left(n+\frac{1}{2}\right) - \frac{2}{\pi}\sum_{m=1}^{\infty}\sum_{p}\sum_{\nu l_p = m}\frac{1}{\nu^2 L_p}\left[\varphi_a^{\gamma_p}\varphi_b^{\eta_p}\varphi_c^{\mu_p} r^{\alpha_p} t^{\beta_p}\right]^{\nu} \times \sin\left[\nu\pi\left(n+\frac{1}{2}\right)\left(\frac{L_p}{L}\right)\right]\sin\left[\nu\pi\left(\frac{L_p}{2L}\right)\right], \tag{66}$$

where γ_p, η_p and μ_p are the number of reflections of the primitive periodic orbit p off V_a, V_b and V_c, respectively.

10. Discussion

Bohr's model of the hydrogen atom (1913) and all subsequent pre-1925 models of atomic and molecular systems are based on the idea of obtaining their spectra by quantizing periodic orbits [18]. It is often suggested that the elimination of periodic orbits from quantum mechanics is one of the central accomplishments of the exact formulation of quantum mechanics by Heisenberg and Schrödinger in 1925/1926. However, it is becoming more and more evident that periodic-orbit quantization is an alternative way of formulating quantum mechanics for

bounded systems. Contrary to the 'old', pre-1925 quantum mechanics, however, all periodic orbits of a quantum system have to be taken into account to obtain exact quantization results. This way periodic-orbit theory reminds us of the ancient Ptolemaic theory of epicycles, a generalized Fourier expansion technique that is exact if an infinite number of cycles are taken into account. In the case of quantum graphs, we have a quantum system that is analytically accessible in every detail and thus illustrates the idea of exact periodic-orbit quantization. Thus, quantum graphs are a paradigm system in periodic-orbit theory and quantum complexity, comparable in importance to the hydrogen atom and the harmonic oscillator in 'conventional' quantum theory.

Periodic-orbit solutions (54) and (66) are a qualitative step forward in several ways. (i) The three-pronged star graph is the first branched quantum graph that has ever been solved explicitly. (ii) A binary symbolic dynamics [18, 19] is no longer sufficient to label the periodic orbits. A ternary symbolic dynamics is necessary, for instance, one consisting of the three symbols A, B and C that refer to the three dead-end vertices V_a, V_b and V_c, respectively. (iii) According to the classification scheme established in [10], the three-pronged star graph is a marginal quantum graph with an order between 0 and 1 that does not satisfy the regularity condition [8, 9]. Such quantum graphs have never before been solved in the literature. Thus, the three-pronged star graph is the highest-order quantum graph that has so far been solved explicitly in terms of exact periodic-orbit expansions. (iv) Since the three-pronged star graph does not satisfy the regularity condition [8], we constructed a new proof of the 'one-root-per-root-cell' property (see section 3). After straightforward adaptation, this proof also works for all zero-order quantum graphs that strictly satisfy the regularity condition. (v) The dynamically regular quantum graphs that have so far been solved in the literature [8, 9, 16] exhibit a non-zero spectral gap $s_n = k_{n+1} - k_n > \kappa > 0$ that prevents us from accessing the small-spacing regime $s \to 0$ when using the explicit spectral formulae as a starting point for statistical investigations of the level spectrum of quantum graphs. The three-pronged star graph is the first explicitly solved quantum graph that allows access to the small-spacing regime.

There are various ways in which the three-pronged star graph, and in fact all finite quantum graphs, may be implemented (approximately) experimentally. We mention implementation of quantum graphs as a network of fiber-optic cables [8] or a network of vibrating guitar strings. The implementation of a quantum graph as a microwave network has already been accomplished in the laboratory [20, 21].

The spectral equation (5) is a member of the class of transcendental, almost-periodic functions [22]. Thus, the explicit solutions derived in this paper contribute to the mathematical problem of computing the zeros of this class of functions.

11. Summary and conclusion

In this paper, we computed explicitly, analytically and exactly the spectrum of the three-pronged star graph. It is surprising that this is possible at all, since, in general, its spectral equation is a transcendental function. While this result extends the frontier of explicitly solved quantum graphs to the marginal ones with order between 0 and 1, the real importance of our work is to serve as a template for further developments in the solution of other quantum systems. In fact, using similar methods, it has recently been possible to solve the spectral problem of the one-dimensional, finite square-well potential [23] and the one-dimensional delta atom [24]. In addition, combining our methods with the spectral hierarchy scheme outlined in [16], the same approach can be used to compute the spectra of quantum star graphs with more than three bonds, explicitly and exactly.

Acknowledgment

ZSP gratefully acknowledges an REU summer stipend from the physics department of Wesleyan University.

References

[1] Kottos T and Smilansky U 1997 *Phys. Rev. Lett.* **79** 4794
[2] Kottos T and Smilansky U 1999 *Ann. Phys., NY* **274** 76
[3] Kuchment P 2004 *Waves Random Media* **14** S107
[4] Gnutzmann S and Smilansky U 2006 *Adv. Phys.* **55** 527625
[5] Pauling L 1936 *J. Chem. Phys.* **4** 673
[6] Ruedenberg K and Scherr C W 1953 *J. Chem. Phys.* **21** 1565
[7] Kottos T and Schanz H 2001 *Physica* E **9** 523
[8] Blümel R, Dabaghian Yu and Jensen R V 2002 *Phys. Rev. Lett.* **88** 044101
[9] Dabaghian Yu, Jensen R V and Blümel R 2001 *JETP Lett.* **74** 235
[10] Dabaghian Yu and Blümel R 2003 *JETP Lett.* **77** 530
[11] Berkolaiko G, Bogomolny E B and Keating J P 2001 *J. Phys. A: Math. Gen.* **34** 335
[12] Berkolaiko G, Keating J P and Winn B 2004 *Commun. Math. Phys.* **250** 259
[13] Keating J P, Marklof J and Winn B 2003 *Commun. Math. Phys.* **241** 421452
[14] Kostrykin V and Schrader R 1999 *J. Phys. A: Math. Gen.* **32** 595
[15] Blümel R, Dabaghian Y and Jensen R V 2002 *Phys. Rev.* E **65** 046222
[16] Dabaghian Yu and Blümel R 2004 *Phys. Rev.* E **70** 046206
[17] Riordan J 1958 *An Introduction to Combinatorial Analysis* (New York: Wiley)
[18] Gutzwiller M C 1990 *Chaos in Classical and Quantum Mechanics* (New York: Springer)
[19] Blümel R and Dabaghian Yu 2001 *J. Math. Phys.* **42** 5832
[20] Hul O, Bauch S, Pakoński P, Savytskyy N, Zyczkowski K and Sirko L 2004 *Phys. Rev.* E **69** 056205
[21] Hul O, Bauch S, Lawniczak M and Sirko L 2007 *Acta Phys. Pol.* A **112** 655
[22] Besicovitch A S 1954 *Almost Periodic Functions* (New York: Dover)
[23] Blümel R 2005 *J. Phys. A: Math. Gen.* **38** L673
[24] Blümel R 2006 *J. Phys. A: Math. Gen.* **39** 8257